DOI: 10.1002/adma.200702134

Indium Nanowires Synthesized at an Ultrafast Rate**

By *Seung Soo Oh, Do Hyun Kim, Myoung-Woon Moon, Ashkan Vaziri, Miyoung Kim, Euijoon Yoon, Kyu Hwan Oh,** and *John W. Hutchinson**

A challenge in the development of nanometer-scale devices, which are envisioned to impact human life in the near future,[1] is the development of economical techniques for the fabrication of their building blocks.[2–5] Owing to their unique and exquisite characteristics,[6–8] nanowires are ideal building blocks for functional nanometer-scale electronics, photonic structures,[9] and nanosurgery devices.[10,11] Here, we report a novel phenomenon that provides a robust technique for fabrication of single-crystal indium nanowires at an ultrafast rate. Indium nanowires have peculiar temperature-dependent electrical properties, which make them attractive for various applications.[12] For example, the electrical resistance of indium nanowires decreases rapidly when reaching the superconducting transition temperature, which makes them more attractive for making magnetic field generators or superconducting quantum interference devices.[13,14] On the other hand, post-processing of indium nanowires (e.g., by oxygen or nitrogen plasma treatment) can be used to create composite nanowires made from indium compound materials on the outer surface layer of the wire. Such composite nanowires have versatile applications in electronics and optoelectronic devices, for example in building biosensors, solar cells, electrodes, and even memory devices.[15–21]

The first step in our experiments is to grow indium-rich InGaN layers of 300 nm thickness epitaxially on an GaN/sapphire substrate having a thickness of 330 μm. Examination of the composition of the fabricated InGaN layers using X-ray diffraction (XRD) (see Experimental) indicated that the layers are ~80% indium. The second step subjects the InGaN layers to direct irradiation by a Ga^+ focused ion beam (FIB). It is observed that FIB irradiation results in rapid growth of straight nanowires on the surface area of the substrate, as shown schematically in Figure 1A. Movie S1 (see Supporting Information) provides an example of the appearance of nanowires as the substrate is subjected to FIB with an ion current density of 400 nA cm^{-2} and an accelerating voltage of 10 kV. From the onset of irradiation, nanowires start to appear after 80 s and grow at an average rate of 50 nm s^{-1} until 260 s, at which point the indium source in the InGaN layer is exhausted as will be explained later. Figure 1B shows four snapshots of the growth sequence for nanowires taken at 50 s time intervals at an ion current density of 200 nA cm^{-2} and an accelerating voltage of 10 kV, where the synthesized nanowires have lengths as long as 30 μm and diameters in the range 50–200 nm.

To examine the material characteristics of synthesized nanowires, we performed transmission electron microscopy (TEM) and energy-dispersive X-ray spectroscopy (EDS). We used these techniques to examine nanowires synthesized at various ion beam accelerating voltages and current densities. Figure 2A and B shows a set of data from these analyses, identifying the synthesized nanowires with diameter smaller than 200 nm as pure indium single crystals. Nanowires with larger diameters are polycrystalline. Moreover, electron energy loss spectroscopy (EELS) analysis was used to investigate the chemical compositions of the nanowires and the surface layer before and after FIB irradiation (Fig. 2C). Prior to FIB irradiation, the InGaN layers are saturated with ~80% indium content of (denoted by red color in Fig. 2C). After irradiation, essentially all the indium is diffused through the substrate pores, producing pure indium nanowires. This can be explained as follows: Upon exposure to Ga^+ FIB, phase decomposition[22,23] occurs in the InGaN with the weaker bond between In and N broken, readily producing

[*] Prof. K. H. Oh, S. S. Oh,[+] D. H. Kim, Prof. M. Kim, Prof. E. Yoon
Department of Materials Science and Engineering
Seoul National University
Seoul, 151-744 (Korea)
E-mail: kyuhwan@snu.ac.kr

Prof. J. W. Hutchinson, Dr. M.-W. Moon, Dr. A. Vaziri
School of Engineering and Applied Sciences
Harvard University
Cambridge, MA 02138 (USA)
E-mail: jhutchinson@fas.harvard.edu

Dr. M.-W. Moon
Future Fusion Technology Laboratory
Korea Institute of Science and Technology
Seoul, 136-791 (Korea)

[+] Present address: Materials Department, University of California, Santa Barbara, CA 93106 (USA)

[**] S.S.O. and D.H.K. contributed equally to this work. The authors thank the Korea Basic Science Institute for HVEM measurements. This work was supported in part by the Ministry of Education through the BK21 Program (K.H.O., M.K., E.Y.), the ERC (Center for Materials and Processes of Self-Assembly) program of MOST/KOSEF (R11-2005-048-00000-0 (E.Y.)) and by a KOSEF grant funded by the Korean government (MOST; No. R01-207-000-10032-0 (D.H.K., K.H.O.) and R0A-2007-000-10014-0 (M.K.)). The work was also supported in part by the KIST project, contract number 2E20200 (M.W.M.), and in part by the School of Engineering and Applied Sciences (A.V., J.W.H.). Supporting Information is available online from Wiley InterScience or from the authors.

ADVANCED MATERIALS

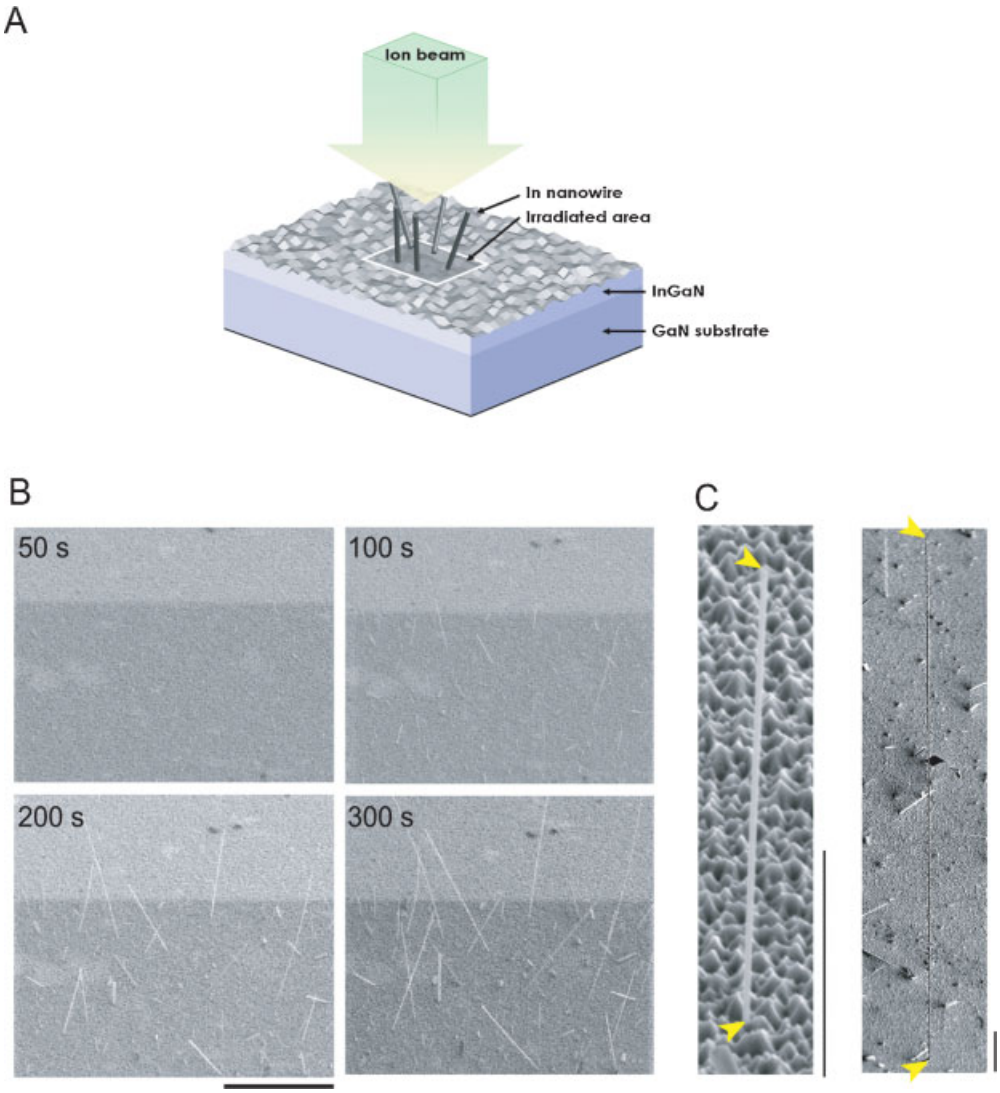

Figure 1. Fabrication of indium nanowires by FIB irradiation. A) Schematic of the experiment. Straight nanowires appear on the surface area of the InGaN layer exposed to FIB. B) Time evolution of formation of straight nanowires after exposure to FIB with an accelerating voltage of 10 kV and an ion current density of 200 nA cm^{-2}. The area subject to FIB is 42×36 μm^2. Scale bar = 20 μm. C) Single nanowires with length and diameter of 20 μm and 100 nm (left) and 130 μm and 300 nm (right) created by FIB irradiation. Arrow heads show the top and bottom of the nanowires. Scale bar = 10 μm.

indium. The indium easily diffuses through pores of the surface layer, while GaN remains in the substrate. It is assumed that the nanowires must grow at the bottom of the wire, where it is attached to the substrate, fed by indium from the substrate. Exhaustion of the indium in the InGaN layer is closely related to the length of the synthesized nanowires. The details of the mechanisms underpinning this phenomenon have not been explored.

In Figure 3, the geometrical characteristics and growth rate of synthesized nanowires have been plotted as a function of Ga^+ ion beam parameters, namely ion current density and accelerating voltage. Figure 3A shows the length of individual straight nanowires synthesized on a 420×360 μm^2 area by FIB irradiation with various accelerating voltages at a fixed ion current density of 15 nA cm^{-2}. At this ion current density, the average length of the synthesized nanowires increases by increasing the accelerating voltage: from 0.503 μm at 5 kV to 60.28 μm at 30 kV (the plot displays that length such that 10% of the wires have equal or larger length). Furthermore, straight nanowires with lengths greater than 100 μm were synthesized at acceleration voltages of 20 kV and 30 kV. The density of indium nanowires, defined as the number of wires per unit area, synthesized at all four accelerating voltages was also estimated (Fig. 3A). At a low accelerating voltage of 5 kV, the nanowire density is ~5.76 μm^{-2}, while for the three other accelerating voltages the nanowire density is at least one order of magnitude lower and decreases by increasing the accelerating voltage. A simple calculation for the total mass of the synthesized nanowires per unit area based on the average diameter and length of the nanowires and the measured density yields 2.20×10^{-2} g m^{-2}

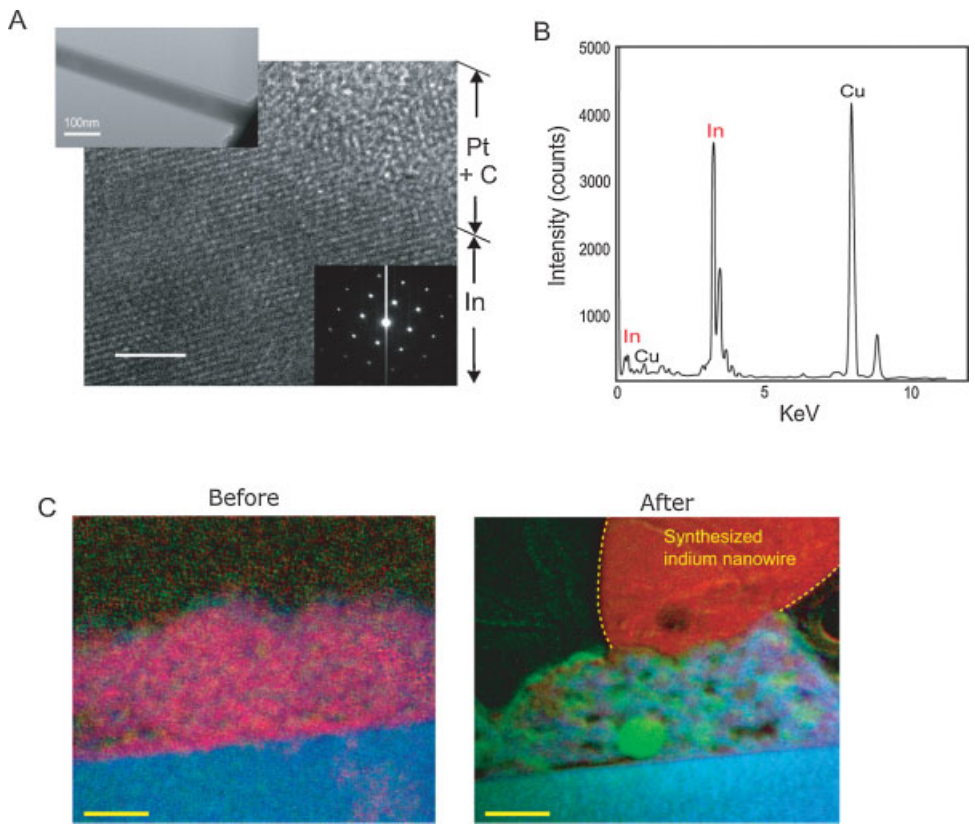

Figure 2. Characterization of synthesized nanowires. A) TEM analysis of the nanowire cross section. Electron diffraction pattern of a nanowire with [110] zone axis confirms that the single crystal grows in the [−1 1 2] direction. The crystal has a body-centered tetragonal structure with lattice constants measured as $a = 0.325$ nm and $c = 0.495$ nm, matching the reported values for bulk indium crystals (Joint Committee on Powder Diffraction Standards (JCPDS) No.5-642). Scale bar = 2 nm. B) EDS spectrum detected in the central region of a cross-sectioned nanowire. The results verify that the wire is pure indium. The presence of copper is believed to result from the Cu TEM grid. C) EELS analysis of InGaN substrate before and after focused ion beam irradiation. The color labels of red, green, and blue denote indium, gallium, and nitrogen, respectively. Prior to ion beam irradiation, over 80% of the InGaN layer is indium (red). After 15 min irradiation by Ga^+ FIB, gallium (green) and nitrogen (blue) were detected below the surface inside the layer, while the indium exists only in the body of the nanowire (red). Scale bar = 100 nm.

and 8.68×10^{-2} g m^{-2} for accelerating voltages of 5 and 30 kV, respectively, which are in the same order of magnitude as the indium content in the surface layer. We further measured the average length and diameter of the synthesized nanowires over a wider range of ion beam parameters. The results are summarized in Figure 3B. The dimensions of the synthesized nanowires depend on the ion beam parameters in a complex fashion. For a current density of 35 nA cm^{-2}, increasing the accelerating voltage leads to thicker and longer indium nanowires, suggesting that the accelerating voltage is closely tied to the driving force in the process. This trend diminishes at higher current densities, since at high accelerating voltage and current density, the Ga^+ ions etch the indium nanowires as well as the InGaN surface. This effect becomes significant at voltages exceeding 20 kV for current densities 350 nA cm^{-2} and higher. In this range the effect of cutting and etching becomes dominant, undermining the growth rate which is driven by accelerating voltage.[24,25]

Finally, the average growth rate of the nanowires was measured over a range of ion beam parameters (Fig. 3C). Here, the growth rate is averaged over 5 distinct sets of experiment, all having the same ion current and accelerating voltage. The measured growth rate is an intricate function of ion beam parameters owing to the complex interplay of the growth and erosion mechanisms discussed above. For example, at the fixed voltage of 10 kV the growth rate increases monotonically from 50 nm s^{-1} to 400 nm s^{-1} as the ion current density is increased from 15 to 7000 nA cm^{-2}. A further increase in the current density led to gradual reduction of the growth rate as the surface of InGaN substrate started to be milled (eroded) by FIB irradiation, resulting in considerable morphological changes of the substrate surface. The maximum growth rate achieved in the range of ion beam parameters in Figure 3C is ~500 nm s^{-1}, at an accelerating voltage of 20 kV and a current density of 2000 nA cm^{-2}. This growth rate is several orders faster than the current techniques (see Fig. 1 and Supporting Information Movie S1).[12,26,27]

As a final step, we controlled the growth region of individual indium nanowires using the method of maskless patterning built into the FIB system. When the InGaN surface is subject to the

ADVANCED MATERIALS

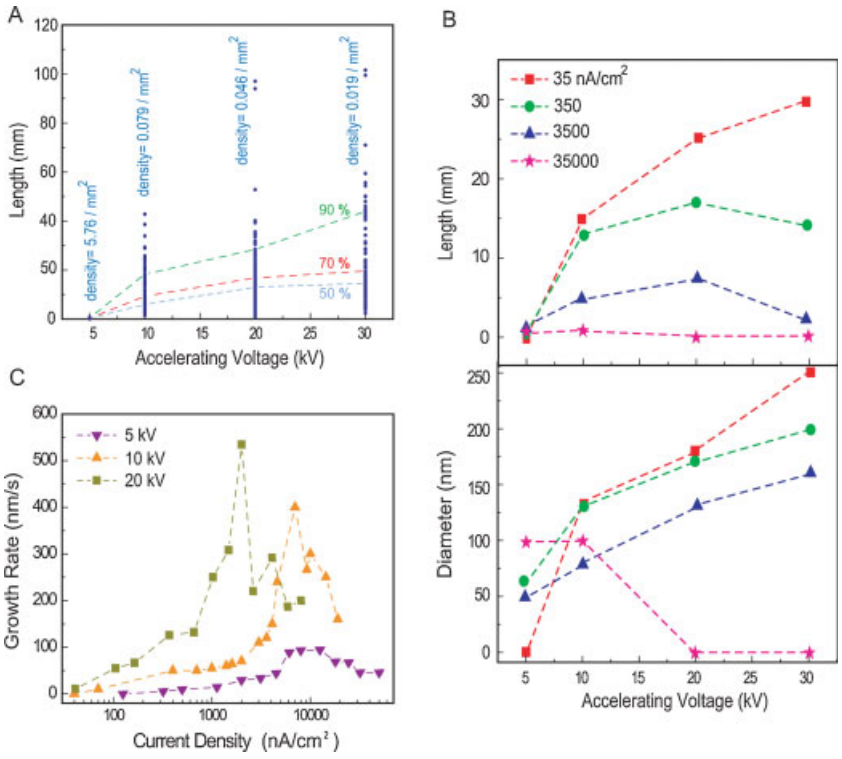

Figure 3. Dependence of the nanowire dimensions and growth rate on the ion beam parameters. A) Length distribution of the nanowires synthesized at a current density of 15 nA cm^{-2} and different ion beam accelerating voltages. The 50% line corresponds to the median of the nanowires length at each accelerating voltage. The lines denoted by 70% and 90% indicate the 70th and 90th percentile of the collected data for nanowire length at each accelerating voltage. The density of the nanowires, defined as the number of nanowires per unit area, is estimated for each case. B) Dependence of the nanowires' average length and diamater on the ion beam parameters. The reported length is the 90th percentile of the collected data. C) Dependence of the average growth rate of the nanowires on the ion beam current density measured for three distinct voltages: 5, 10, and 20 kV. Here, the average growth rate for each nanowire is estimated as the total length divided by total growth time.

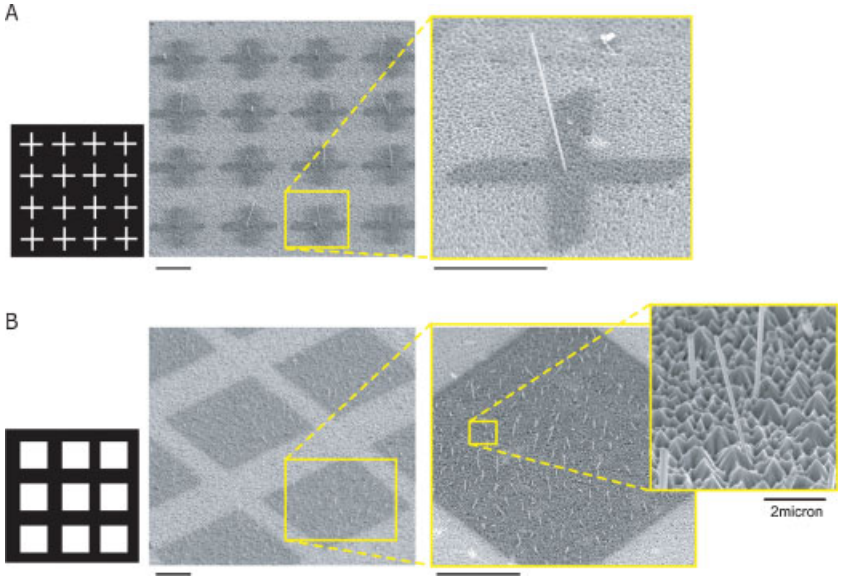

Figure 4. Functional networks of nanowires. A) SEM image of a network of single indium nanowires created on selected locations of the InGaN layer using a maskless patterning method. A bitmap with crossed bars of 500 nm width and 12.5 μm length with the desired pattern (shown on left) were imported to the FIB such that only the white regions were exposed to the ion beam. B) Nanowire forests of 25 × 25 μm^2 size. The synthesized nanowires have an average length and diameter of 2–3 μm and 50 nm, respectively (right of (B)). In both experiments, the current density and accelerating voltage of the ion beam were 1.2 μA cm^{-2} and 10 kV for (A) and 350 nA cm^{-2} and 5 kV for (B). (See Supporting Information Movie S2). Scale bar = 5 μm, unless denoted otherwise.

cross-shaped FIB irradiation shown in Fig. 4A, single nanowires emerge and grow at the center of the irradiated areas due to FIB overlapping.[28] In this set of experiments, the ion beam was raster-scanned over the cross-shaped area from left to right and from top to bottom, leading to increased ion concentration at the center of the cross-shaped region. This method enables selection of the site of growth of individual nanowires. In Fig. 4A the current density and accelerating voltage are 1.2 μA cm^{-2} and 10 kV, which results in indium nanowires with an average diameter and length of 80 nm and 6 μm, respectively. The average growth rate is 30 nm s^{-1} in this case. This method of creation of well-defined functional networks of nanowires has a significant potential in a number of scientific fields and technological applications, such as electronics and optoelectonic devices.[5,15–21] Owing to their low melting point, site-controlled indium nanowires can be also used for assisting the growth of aligned long nanotubes using vapor–liquid–solid mechanisms.[28–30] This method can be used for building nanothermometer devices, opening avenues for designing novel temperature-driven switches and sensors.[17,31] Furthermore, using the maskless patterning method, we have created blocks of 25×25 μm^2 nanowire forests (Fig. 4B). In this case a Ga^+ ion beam with accelerating voltage and current density of 5 kV and 350 nA cm^{-2}, respectively, was raster-scanned over areas of the substrate. The fabricated nanowires have average length and diameter of 2–3 microns and 50 nm, respectively.

In conclusion, we provide a method for controlled fabrication of straight indium nanowires on selected areas of the substrate. The growth rate of nanowires in this method is much higher than growth rates available by currently techniques. Extension of the developed technique allows for fabrication of variety of functional networks of indium nanowires, with control over individual nanowires sites and dimensions. We briefly outlined potential implications of the developed technique, which can impact the current state of the art for building functional nanodevices.

Experimental

Preparation of InGaN layer: Indium-rich InGaN layers of 300 nm thickness were grown epitaxially on a GaN/sapphire substrate with thickness 330 μm at 650 °C by metal–organic chemical vapor deposition (MOCVD). Trimethylgallium (TMGa), trimethylindium (TMIn), and ammonia were used as Ga, In, and N sources, respectively, and the input flow rates of TMGa, TMIn, and NH_3 were 1.5 sccm, 225 sccm and 3 slm, respectively. Synthesized InGaN layers were saturated with ~80% indium, confirmed by XRD, and its roughness (root-mean-square) was measured as 30 nm using atomic force microscopy (AutoProbe CP research system, ThermoMicroscopes).

Focused Ion Beam Irradiation: Indium-rich InGaN layers were exposed to FIB of Ga^+ ion with various ion current densities and accelerating voltages at room temperature using high-resolution FIB/FE-SEM dual-beam system equipped with a Ga liquid metal source (Nova NanoLab 200, FEI). The pressure range inside the vacuum chamber was maintained within 2.0×10^{-4} to 6.0×10^{-4} Pa during the experiment. During exposure to FIB, the formation of nanowires was monitored in situ by a FE-SEM system.

Characterization of Synthesized Nanowires: For performing TEM analysis, a target single nanowire was isolated from the InGaN layer by a manipulation probe (Model 100.7, Omniprobe). The thickness of nanowires was reduced to 5–60 nm by milling using FIB for the analysis by TEM and EDS. This procedure was performed at the temperature of −90 °C, using a cooling stage to prevent the nanowire from melting with high temperature during milling. Then, the cross-section of the nanowires with the thickness ~60 nm was examined using TEM (JEM-3000F, JEOL). The chemical composition of the nanowires was analyzed using energy-dispersive X-ray spectroscopy (EDS, OXFORD). The structural properties of nanowires were confirmed by high-resolution TEM and electron diffraction patterns. The compositional change of InGaN layer during FIB irradiation was examined by electron energy loss spectroscopy (EELS) using high-voltage electron microscopy (HVEM, JEOL).

Creation of Functional Networks of Nanowires: Functional networks of individual nanowires were created by adopting the maskless patterning method of the FIB equipment. This method permits the accurate selection of the areas exposed to FIB. The bitmap file of the exposure pattern was imported as a virtual mask in the FIB system. The ion beam was raster-scanned over the cross-shaped area with dwell time of 1 μs.

Received: August 23, 2007
Revised: November 13, 2007
Published online: February 29, 2008

[1] C. M. Lieber, *MRS Bull.* **2003**, *28*, 486.
[2] Y. Xia, P. Yang, Y. Sun, Y. Wu, B. Mayers, B. Gates, Y. Yin, F. Kim, H. Yan, *Adv. Mater.* **2003**, *15*, 353.
[3] H. J. Fan, P. Werner, M. Zacharias, *Small* **2006**, *2*, 700.
[4] F. Patolsky, B. P. Timko, G. Zheng, C. M. Lieber, *MRS Bull.* **2007**, *32*, 142.
[5] A. Javey, S. Nam, R. S. Friedman, H. Yan, C. M. Lieber, *Nano Lett.* **2007**, *7*, 773.
[6] A. K. Geim, I. V. Grigorieva, S. V. Dubonos, J. G. S. Lok, J. C. Maan, A. E. Filippov, F. M. Peeters, *Nature* **1997**, *390*, 259.
[7] A. P. Alivisatos, P. F. Barbara, A. W. Castleman, J. Chang, D. A. Dixon, M. L. Klein, G. L. McLendon, J. S. Miller, M. A. Ratner, P. J. Rossky, S. I. Stupp, M. E. Thompson, *Adv. Mater.* **1998**, *10*, 1297.
[8] J. Hu, T. W. Odom, C. M. Lieber, *Acc. Chem. Res.* **1999**, *32*, 435.
[9] R. Agarwal, C. M. Lieber, *Appl. Phys. A* **2006**, *85*, 209.
[10] I. Obataya, C. Nakamura, S. Han, N. Nakamura, J. Miyake, *Nano Lett.* **2005**, *5*, 27.
[11] G. Zheng, F. Patolsky, Y. Cui, W. U. Wang, C. M. Lieber, *Nat. Biotechnol.* **2005**, *23*, 1294.
[12] G. Yi, W. Schwarzacher, *Appl. Phys. Lett.* **1999**, *74*, 1746.
[13] N. Giordano, *Phys. Rev. Lett.* **1988**, *61*, 2137.
[14] M. Tinkham, in: *Introduction to Superconductivity*, 2nd ed.,McGraw-Hill, New York **1996**.
[15] S. Vaddiraju, A. Mohite, A. Chin, M. Meyyappan, G. Sumanasekera, B. W. Alphenaar, M. K. Sunkara, *Nano. Lett.* **2005**, *5*, 1625.
[16] G. Cheng, E. Stern, D. Turner-Evans, M. A. Reed, *Appl. Phys. Lett.* **2005**, *87*, 253103.
[17] Y. Li, Y. Bando, D. Golberg, *Adv. Mater.* **2003**, *15*, 581.
[18] D. Zhang, Z. Liu, C. Li, T. Tang, X. Liu, S. Han, B. Lei, C. Zhou, *Nano. Lett.* **2004**, *4*, 1919.
[19] P. Nguyen, H. T. Ng, T. Yamada, M. K. Smith, J. Li, J. Han, M. Meyyappan, *Nano. Lett.* **2004**, *4*, 651.
[20] J. Wang, M. S. Gudiksen, X. Duan, Y. Cui, C. M. Lieber, *Science* **2001**, *293*, 1455.
[21] H. Pettersson, J. Trägårdh, A. I. Persson, L. Landin, D. Hessman, L. Samuelson, *Nano. Lett.* **2006**, *6*, 229.
[22] J. Lian, W. Zhou, Q. M. Wei, L. M. Wang, L. A. Boatner, R. C. Ewing, *Appl. Phys. Lett.* **2006**, *88*, 093112.

[23] A. Lugstein, B. Basnar, E. Bertagnolli, *Nucl. Instrum. Methods Phys. Res., Sect. B* **2004**, *217*, 402.
[24] A. A. Tseng, *Small* **2005**, *1*, 924.
[25] L. Frey, C. Lehrer, H. Ryssel, *Appl. Phys. A-Mater. Sci. Process.* **2003**, *76*, 1017.
[26] C. Y. Nam, J. Y. Kim, J. E. Fischer, *Appl. Phys. Lett.* **2005**, *86*, 193112.
[27] K. Soulantica, A. Maisonnat, F. Senocq, M.-C. Fromen, M.-J. Casanove, B. Chaudret, *Angew. Chem. Int. Ed.* **2001**, *40*, 2984.
[28] R. Buckmaster, T. Hanada, Y. Kawazoe, M. Cho, T. Yao, N. Urushihara, A. Yamamoto, *Nano. Lett.* **2005**, *5*, 771.
[29] S. D. Dingman, N. P. Rath, P. D. Markowitz, P. C. Gibbons, W. E. Buhro, *Angew. Chem. Int. Ed.* **2000**, *39*, 1470.
[30] Y. Li, Y. Bando, D. Golberg, *Adv. Mater.* **2004**, *16*, 37.
[31] J. Zhan, Y. Bando, J. Hu, Z. Liu, L. Yin, D. Golberg, *Angew. Chem. Int. Ed.* **2005**, *44*, 2140.

